# THz Multi-pulse Sequence Generating System Using Interferometric Light-Beating Setup

by

Kai Shuen Tan

A senior thesis submitted in partial fulfillment

of the requirements for the degree of

Honors Bachelor of Science

(Physics)

in The University of Michigan

2011

## ACKNOWLEDGEMENTS

I would like to thank my research advisor, professor Hui Deng for giving me the opportunity to perform research in her group. I thank her for the time she spent patiently giving me guidance and assistance in completing various projects. I would also like to thank Paul Bierdz, a graduate student in my group who had helped me immensely in my research project. I thank him for the hours he spent weekly in helping me with my setup and guiding me in my research project. Finally, I thank all the other group members who helped in creating a fun and intellectual working environment.

# Table of Contents

Abstract

Theoretical Background

I. Microcavity Exciton-Polaritons

II. Photoluminescence Measurements

a) Angle-resolved measurements

b) Temporal measurements

Characteristics of the Pump Beam Pulse

Interferometric Light Beating Setup

a) Diffraction gratings

b) Wavelength selection

c) Pulse beating

Detecting Signals

Problems with the Setup and Improvements Made

Conclusion

References

## Abstract

Electronic pulse generators could typically generate pulses with pulse width in the range of hundreds of picoseconds to several thousand seconds. In the lower limit, some of the more advanced pulse generators in the market could generate pulses with width of several hundred picoseconds. However, at the lower limit of pulse width, the jitter from the electronics also become significant, with some of them having jitter on the order of tens of picoseconds. The prices of pulse generators that are able to generate pulses in limit of several hundred of picoseconds are also expensive. For example, Berkeley Nucleonics Corporation's Model 575 8-channel pulse generator has a pulse width resolution of 250ps, 50ps jitter and can produce pulse sequence of up to 8 pulses. This model sells for $5160 as of the date this thesis is written [1]. Another similar model from Quantum Composers is 9350 Series 8-channel pulse generator. This generator has pulse width resolution of 250ps, less than 50ps jitter and can produce pulse sequence of up to 8 pulses. This model sells for $5418 as of the date this thesis is written [2].

As discussed, for low pulse width generation, electronic pulse generators in the market are expensive and also have significant jitter. More importantly, the pulse width generated from these pulse generators also does not meet the requirement of our group. For our group purposes, picoseconds pulse sequences are required to study the dynamics of the samples used. Using lab techniques, several methods were employed to modulate femto-second and pico-second pulses to give a multi-pulse sequence with desired pulse width (and delay time) between pulses. The theory of these methods as well as the results collected in our lab will be presented in this paper.

## Theoretical Background:

Before developing a multi-pulse sequence generating system for my group, it is important to first understand the characteristics of the sample that this setup was designed. Next, it is also important to understand the types of measurements that will be made on the sample so that the setup could be designed for the different types of measurements.

### I. Microcavity Exciton-Polariton

One of the research interests of my group is to develop a quantum well microcavity to study the physics of an exciton-polariton system. By placing GaAs quantum wells at the antinodes of the semiconductor microcavity and applying an optical field, the heavy hole excitons from the semiconductor would be able to strongly interact with the optical field. If energy transfer between the cavity and the excitons are much faster than the decoherence rates and decay of both the cavity photons and excitons, then the coupling of photon and exciton would form a new "quasi-particle" called polaritons. [3]

Using rotating wave approximation, the Hamiltonian of the system described above could be written as:

$$\widehat{H}_{pol} = \widehat{H}_{cav} + \widehat{H}_{exc} + \widehat{H}_{I}$$

$$\widehat{H}_{pol} = \sum E_{cav}(k_{\parallel}, k_c)\hat{a}^{+}_{k_{\parallel}}\hat{a}_{k_{\parallel}} + \sum E_{exc}(k_{\parallel})\hat{e}^{+}_{k_{\parallel}}\hat{e}_{k_{\parallel}} + \sum \hbar\Omega(\hat{a}^{+}_{k_{\parallel}}\hat{e}_{k_{\parallel}} + \hat{a}_{k_{\parallel}}\hat{e}^{+}_{k_{\parallel}}) \qquad (1)$$

where $a^{+}_{k_{\parallel}}$ is the photon creation operator with inplane wavenumber $k_{\parallel}$, $\hat{e}^{+}_{k_{\parallel}}$ is the exciton creation operators with inplane wavenumber $k_{\parallel}$ and $\hbar\Omega$ is the exciton-photon dipole interaction

energy. $E_{cav}$ is the cavity resonant energy and $E_{exc}$ is the exciton energy. From equation (1), the third term on the right hand side gives the photon and exciton interaction through the optical field. The Hamiltonian in equation (1) however, is not diagonalized. To diagnolize it, the following transformations are made:

$$\hat{p}_{k_\parallel} = X_{k_\parallel}\hat{e}_{k_\parallel} + C_{k_\parallel}\hat{a}_{k_\parallel} \tag{2}$$

$$\hat{q}_{k_\parallel} = -C_{k_\parallel}\hat{e}_{k_\parallel} + X_{k_\parallel}\hat{a}_{k_\parallel} \tag{3}$$

With these transformations the diagonalized Hamiltonian is as follows:

$$\hat{H}_{pol} = \sum E_{LP}(k_\parallel)\hat{p}^{+}_{k_\parallel}\hat{p}_{k_\parallel} + \sum E_{UP}(k_\parallel)\hat{q}^{+}_{k_\parallel}\hat{q}_{k_\parallel} \tag{4}$$

where $(\hat{p}^{+}_{k_\parallel}\hat{p}_{k_\parallel})$ and $(\hat{q}^{+}_{k_\parallel}\hat{q}_{k_\parallel})$ are the two eigen-modes of the system with eigen-energies $E_{LP}$ and $E_{UP}$ respectively. These two modes are known as lower polaritons (LP) and upper polaritons (UP). From equation (2) and (3), it can be seen that the LP and UP are just linear superposition of excitons and photons with same inplane wavenumber $k_\parallel$ with the population of excitons and photons given by the square of the coefficients, $X_{k_\parallel}$ and $C_{k_\parallel}$. From equation (4), the eigen-energies could be solved and are given by:

$$E_{UP}(k_\parallel) = \frac{1}{2}\left[E_{exc} + E_{cav} - \sqrt{4\hbar^2\Omega^2 + (E_{exc} - E_{cav})^2}\right] \tag{5}$$

$$E_{LP}(k_\parallel) = \frac{1}{2}\left[E_{exc} + E_{cav} + \sqrt{4\hbar^2\Omega^2 + (E_{exc} - E_{cav})^2}\right] \tag{6}$$

The minimum energy separation between the lower polariton and upper polariton states are given by $E_{UP} - E_{LP} = 2\hbar\Omega$, this energy splitting is known as 'Rabi splitting'. From equation (5) and (6), it can be seen that by tuning the exciton energy far away from the Rabi energy, i.e $|E_{exc} -$

$E_{cav}| \gg \hbar\Omega$, then equation (5) reduces to the exciton energy and equation (6) reduces to the cavity energy.

Thus, the concept of polaritons is most useful when the exciton energy and the cavity energy are comparable, and the coupling between the exciton and photon is strongest at Rabi energy.

However, the most important parameter for this research is the lifetime of the polaritons. In terms of the lifetime of exciton and cavity, equation (5) and (6) can be rewritten as:

$$E_{LP}(k_{\parallel}) = \frac{1}{2}\left[E_{exc} + E_{cav} + i(\gamma_{cav} + \gamma_{exc}) + \sqrt{4\hbar^2\Omega^2 + [E_{exc} - E_{cav} + i(\gamma_{exc} - \gamma_{cav})]^2}\right] \quad (7)$$

$$E_{UP}(k_{\parallel}) = \frac{1}{2}\left[E_{exc} + E_{cav} + i(\gamma_{cav} + \gamma_{exc}) - \sqrt{4\hbar^2\Omega^2 + [E_{exc} - E_{cav} + i(\gamma_{exc} - \gamma_{cav})]^2}\right] \quad (8)$$

where $\gamma_{cav}$ is the out-coupling rate of a cavity photon due to imperfect mirrors, and $\gamma_{exc}$ is the non-radiative decay rate of an exciton.

As polariton is a linear superposition of exciton and photon, similarly, the lifetimes of polaritons can also be expressed as a linear superposition of the lifetimes of exciton and photon.

$$\gamma_{LP} = |X|^2\gamma_{exc} + |C|^2\gamma_{cav} \quad (9)$$

$$\gamma_{UP} = |C|^2\gamma_{exc} + |X|^2\gamma_{cav} \quad (10)$$

The polaritons lifetimes are mainly given by the cavity lifetime. For the sample used in our group, the polaritons lifetime is on the order of a few picoseconds.

## II. Photoluminescence measurements

Photoluminescence (PL) is a process in which a substance absorbs and then re-radiates a photon. There are two types of PL measurements that could be made on the sample our group used. The first is angle-resolved measurements and the second is time-resolved measurements.

### a) Angle-resolved measurements

Figure I. below shows a typical setup used for angle-resolved measurements.

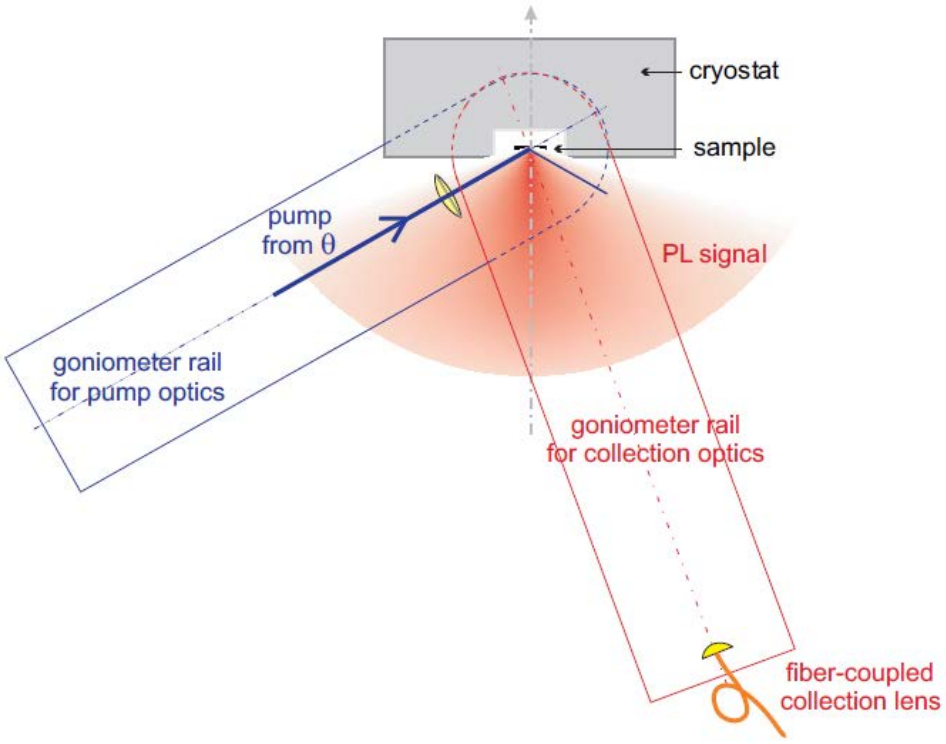


*Figure 1. Experimental setup for angle-resolved measurement* [3]

As seen from figure 1, there are two parts to the setup, the pump optics and the collection optics. Using the multi-pulse generating setup, the laser pulses generated would be sent from an angle θ measured with respect to the normal of the sample. The pulses are then focused to the sample using a doublet lens. The emission signal from the sample is then collected by a fiber-coupled

collection lens, which are then connected to a spectrometer. Both the pump and collection optics are mounted on extended goniometer rails centered about the sample. The goniometer rails can then be used to vary the pump angle as well as the collection angle. For a given pump angle, by varying the collection angle, the intensities of the emitted radiation could be found at different angles which corresponds to the different $k_{\parallel}$ of the sample. Using this data, the polaritons energy dispersion can be plotted for this pump angle. By varying the pump angle, the detuning of the system is also varied, and the energy dispersion plots can be found for the different detunings. The data collected using this method can be fitted with the theoretical curve given by equation (5) and (6), and different parameters of the system can be determined from the fit. For example by using the $2\hbar\Omega$ and $E_{exc}$ as the free parameters, both of these values can be found from fitting the curve to different energy dispersion curves.

b) Temporal measurement

There are two types of temporal measurements that could be made on the sample. First, using a streak camera, time-resolved measurements can be made. Second, using an autocorrelator, the intensity correlation measurements can be made.

A streak camera measures the variation in the intensity of a pulse with time. Typically, a streak camera has resolution on the order of a few picoseconds. By sending the signal to the streak camera, the temporal distribution of the signal could be found.

An autocorrelator measures the intensity correlation of a pulse with itself as a function of time separation between them. The intensity correlation of a signal is given by:

$$I(\tau) = \int P(t)P(t+\tau)dt \qquad (11)$$

From the autocorrelation signal, the pulse duration and the waveform of the original signal could be determined.

**Characteristics of the pump beam pulse**

For both types of PL measurements, single and multi-pulse train could be used as the pump beam. The type of pulse train to use depends on what types of system dynamics that will be studied. The parameters of the pulse such as time duration and the carrier frequency of the pulse also depend on the characteristics of the sample.

The first case of pump beam to consider is the simplest one in which a continuous wave is sent as the pump beam. After a while, the system will reach a steady state in which the net transfer of energy in the system is zero.

The second case of pump beam to consider is single-pulse train in which the pulse duration is comparable to or smaller than the lifetime of polariton. After the pulse was pumped into the system, some of the cavity photons and excitons will be in the excited state and the relaxation dynamics of the system can be studied. If instead a pulse has duration much larger than the lifetime of polariton, then the pulse beam approaches a continuous wave as in first case.

The third case of pump beam to consider is also the main interest of this research is a multi-pulse train pump beam. The pulse duration used is the same as in the second case, but the delay time between the successive pulse is also on the order of the lifetime of the polaritons.

For the second case, if the single-pulse train was sent directly from the laser source, then the delay time of successive pulses is determined by the repetition rate of the laser. For a typical

mode-locked pulse from a Ti-Sapphire laser, the repetition rate is ~80MHz, corresponding to a delay time of ~13ns. This delay time is about 2 orders larger than the relaxation time of the polaritons, thus the system would return to its equilibrium state before the next incident pulse. A multi-pulse train in contrast tries to probe the non-equilibrium relaxation dynamics of the system.

**Interferometric light-beating setup**

There are several ways possible to generate a multi-pulse sequence. In this research, an intereferometric light beating setup was used.

The basic idea of this setup is to generate beats from two pulses differing slightly in wavelength. The resulting pulse from the beating is a pulse envelope consisting of several periods of amplitude varying sinusoidal wave.

The general picture of the setup is shown in figure 2 below. This setup is similar to a Mach-Zehnder interferometer where a beam is split into two using a beamsplitter and recombined using another beamsplitter. As a result of the interference of the two pulses that were recombined, beats will be produced.

The wavelength selectors in the two paths were used to select two bands of wavelength with angular frequency $\omega_1$ and $\omega_2$. A delay stage was set in one of the pulse paths to vary the relative phase between the pulses. After the pulse was recombined at the second beamsplitter, one port of the beam splitter sends the output pulse to a detector to measure the beat signal while the other port of the beam splitter sends the output pulse to the sample as the pump beam.

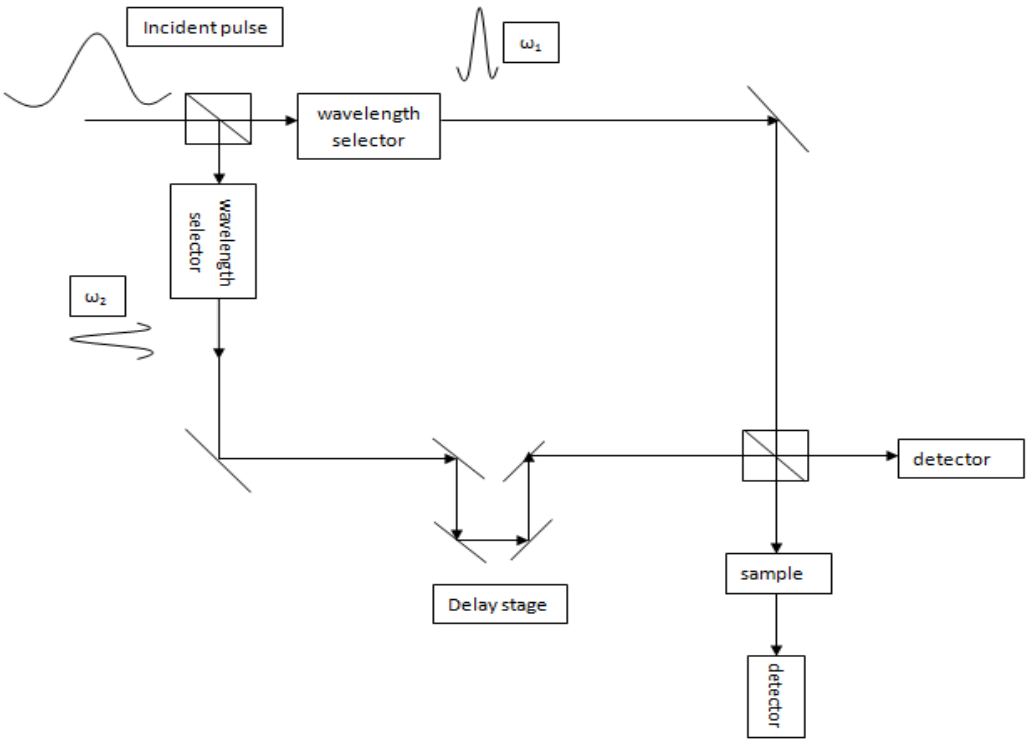


*Figure 2. General setup of an interferometric light beating setup*

The actual setup in the lab used a 100fs mode-locked incident pulse of wavelength $\lambda = 750nm$ as the incident pulse. As for the wavelength selector, two 1800 groves/mm diffraction gratings and two variable slits were used to select the wavelengths.

a) Diffraction gratings

The diffraction equation is given by:

$$\sin(\theta_i) + \sin(\theta_m) = \frac{m\lambda}{a} \tag{12}$$

where m is the diffraction mode, a is the spatial period of the gratings, $\theta_i$ is the incident angle of the light and $\theta_m$ is the diffraction angle of the light for mode m. In general, the diffraction gratings will diffract light into several modes, m according to the relation given by equation (12).

However, for minimum power loss, the diffraction equation should only admit two solutions. Since the left hand side of equation (12) cannot sum to more than 2, then for equation (12) to admit only 2 modes, the following conditions have to be satisfied:

$$\frac{2\lambda}{a} < 2 \tag{13}$$

$$\frac{3\lambda}{a} > 2 \tag{14}$$

The m=0 mode corresponds to the reflection mode. If m=0 is substituted into equation (12), then the law of reflection is recovered with index of refraction equals to 1. In the m=0 mode, the incident light is simply reflected but not diffracted. The m=1 mode is the first order diffraction mode. Rearranging equation (12), then the first order diffraction angle is given by:

$$\theta_1 = \sin^{-1}(\frac{\lambda}{a} - \sin(\theta_i)) \tag{15}$$

From equation (15), it can be seen that the diffraction angle is increasing in wavelength. Thus for an incident pulse with a range of wavelength within the pulse, the diffracted light will be dispersed spatially following the relation given by equation (15).

b) Wavelength selection

For wavelength selection, a setup as shown in figure 3 was used.

This setup is similar to a 4-f imaging setup. The dispersed laser beam from the m=1 diffraction mode was focused using a cylindrical lens. A cylindrical lens was used because it could focus the beam in the transverse plane that will be useful for wavelength selection.

Using a beam splitter, the focusing beam was split into two. A variable slit was placed in each of the Fourier plane of the lenses (1 focal length away from the cylindrical lens). The slit was used to select bands of pulses from the incident pulse. Using another set of cylindrical lens, the two bands of pulses selected were re-collimated.

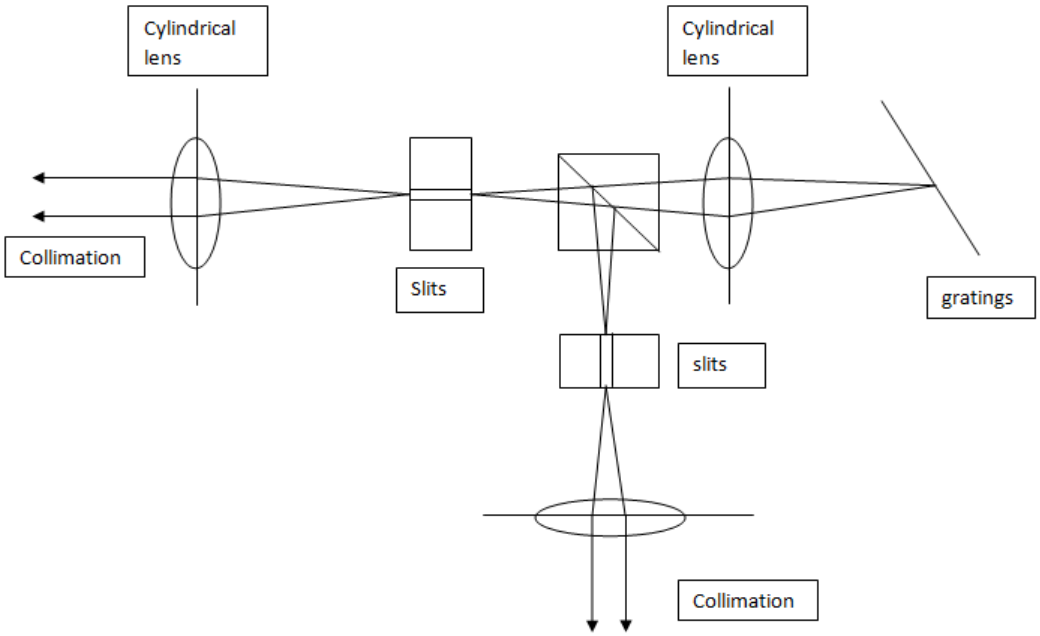


*Figure 3. Setup for wavelength selection*

The Fourier transform of the pulse beam is given by:

$$x = \lambda f \nu_x \tag{16}$$

where x is position of the beam in its transverse direction in the Fourier plane, f is the focal length of the lens and $\nu_x$ is the spatial frequency of the diffraction gratings. The product of $f\nu_x$is a constant. Thus as seen from equation (16), the different components of the wavelength are dispersed spatially in the Fourier plane. Since the beam is focused in the transverse direction,

then a slit placed in the Fourier plane would be able to select a band from the incident pulse. In the lab, a variable slit was used. The smallest slit width that could be adjusted to was ~10μm.

Using a 100fs pulse that has a full width at half maximum (FWHM) of about ~10nm, the two bands with central frequency $\omega_1$and $\omega_2$ were selected from the incident pulse.

Figure 4 below shows a screenshot of the two bands of pulses from the spectrometer.

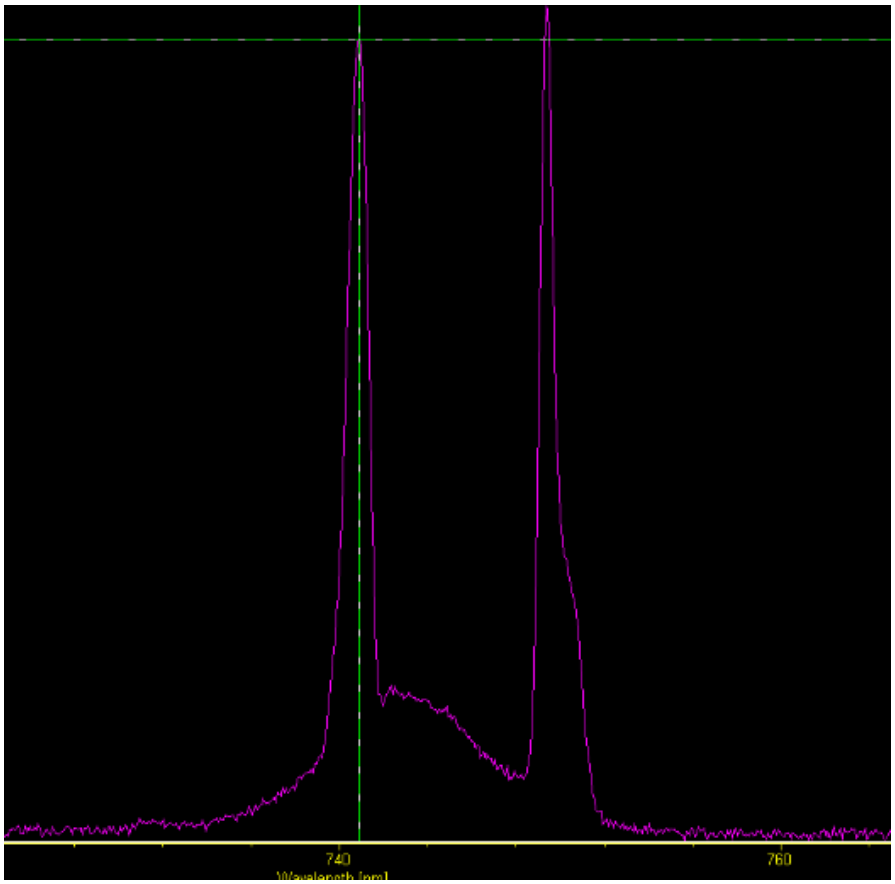


*Figure 4. Intensity plot from spectrometer showing the two peaks that correspond to the two bands selected by the variable slits from the incident 100fs pulses.*

c) Pulse beating

Finally using mirror to direct the beam and a retroreflector to vary the pathlength of one of the beams, the two beams are recombined with another beamsplitter. For the two pulses to beat, the two pulses will have to overlap spatially. The two paths should have almost exactly the same path length. Using the retroreflector, finer adjustments on the path length can be made.

**Detecting beating signals**

If the difference in wavelength for the two pulses is ~2nm, then this correspond to a beating frequency of ~1THz. With the delay time between the two beats given by the laser source repetition time, it was ~12.5ns. The beating signal produced using these parameters should have waveform similar to that shown in figure 5 below.

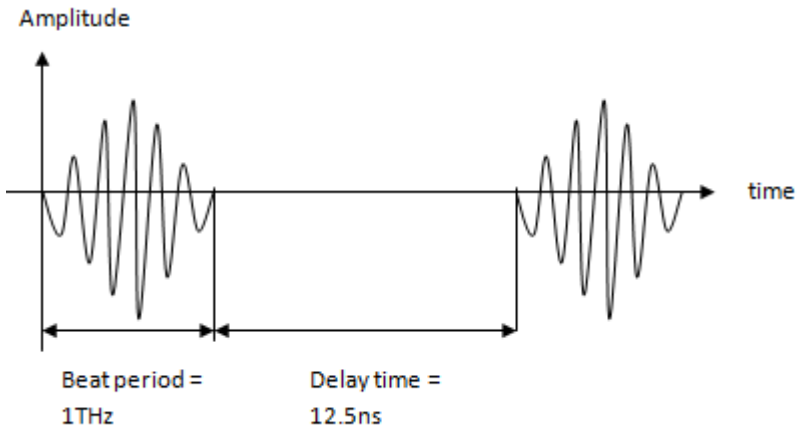


*Figure 5. Waveform of beating signal from with beat period 1THz and a delay time of 12.5ns between successive beat envelopes.*

In the lab, the beating signal was measured using autocorrelator, and the intensity information of the signal was recorded. The intensity of the signal was found by squaring the amplitude of the wave. So, ideally, the intensity plot should look like figure 6 below.

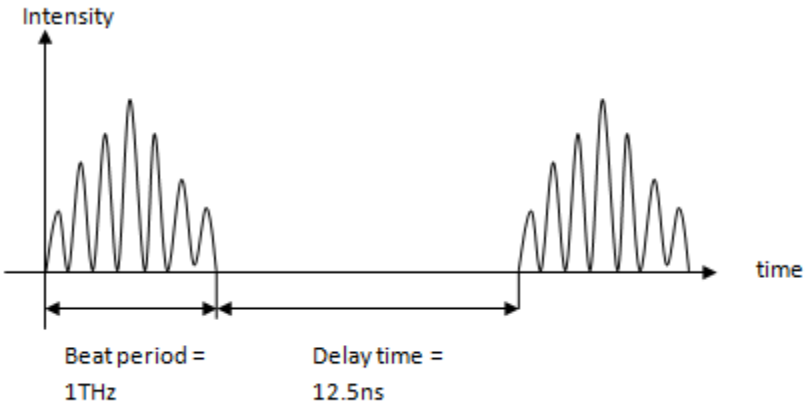


*Figure 6. Intensity plot of beating signal with beat period 1 THz and a delay time of 12.5ns between successive beat envelopes.*

The result of the signal measured in the lab using an autocorrelator is shown below in figure 7.

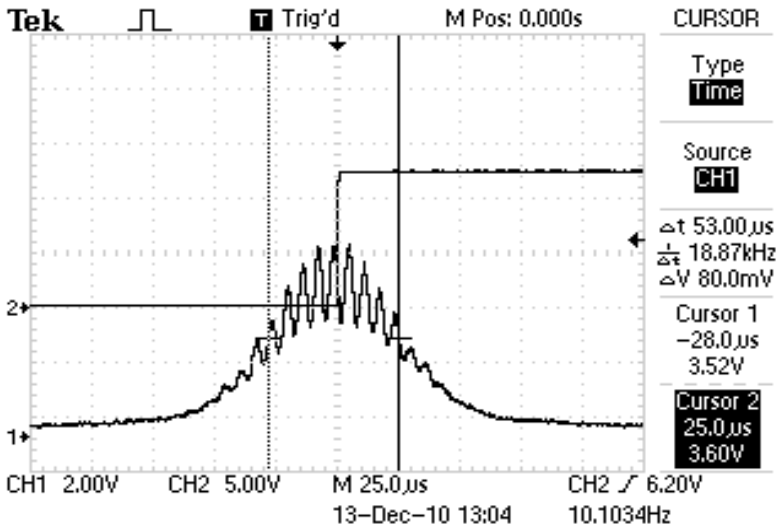


*Figure 7. Output on oscilloscope screen for the signal detected by autocorrelator*

As seen in figure 7, beating signals were indeed detected. However, the dips did not go all the way down to the bottom of the waveform. This indicated that the visibility of the signal was not very good. The rather poor visibility of the signal was mainly due to the misalignment of some of the optics. This was confirmed by shifting slightly some of the optics and the visibility of the signal changed quite significantly.

**Problems with the setup and improvements made**

Since this setup was built before a good understanding was gained about the types of measurements that will be made on the sample, the resulting beating signals do not meet some of the requirements needed to be used as a pump beam.

For instance, since the streak camera will be used for the temporal measurements of the signals, and the highest resolution of the streak camera is ~1-3ps. Then the beating period should be on the order of tens of picoseconds, and the periods within the beating envelope should be on the order of a few picoseconds so that the streak camera would be able to resolve the signal.

However, the beating signal has beating period produced with the setup discussed above has beating period of ~1ps, about an order less than what was needed.

To remedy this, the setup was reconstructed in the lab with the beam expanded before the diffraction gratings. A smaller slit width of ~5μm was also used. However, since the setup was still incomplete as of the date this thesis was written, no data has been taken from the new setup.

## Conclusion:

Using the interferometric light-beating setup, the desired multi-pulse sequence was obtained. This setup has the advantage that it has several parameters of the pulse that can be varied easily once the setup was built. For example, the beating period and the carrier frequency of the pulse can be changed by changing the bands selected and adjusting the central wavelength of the laser source.

However, further improvements can still be made on the setup as discussed to meet the requirement needed for use as a pump beam.

# References

[1] *BNC | Products | Model 575 Digital Delay / Pulse Generator*. Web. <http://www.berkeleynucleonics.com/products/model_575.html>.

[2] "Digital Pulse Generator and Delay Generator Manufacturer." *Quantum Composers - Pulse Generator Technology*. Web. <http://www.quantumcomposers.com/products/pulse-generators/9530-pulse-generator>.

[3] Deng, H., *Dynamic condensation of semiconductor microcavity polaritons*, thesis (Ph.D.), Stanford University. (2006)

[4] Saleh, Bahaa E. A., and Malvin Carl. Teich. *Fundamentals of Photonics*. Hoboken, [u.a.: Wiley-Interscience, 2007. Print.

[5] *RP Photonics Consulting - Laser and Amplifier Design, Nonlinear Optics, Fiber Optics, Fiber Lasers and Amplifiers, Ultrashort Pulses, Optoelectronics, Consultant, Training*. Web. <http://www.rp-photonics.com/>.